

Ferroelectric Properties of $\text{Bi}_{0.5}(\text{Na}_{0.8}\text{K}_{0.2})_{0.5}\text{TiO}_3$ Ceramics

Javier Camargo^{1,a}, Leandro Ramajo^{1,b}, Fernando Rubio-Marcos^{2,c}, Miriam Castro^{1,d*}

¹Institute of Research in Materials Science and Technology (INTEMA), Juan B. Justo 4302 (B7608FDQ), Mar del Plata, Argentina

²Institute of Ceramic and Glass (ICV), Campus UAM c/Kelsen 5, Madrid, Spain

^ajavijec@gmail.com, ^blramajo@fi.mdp.edu.ar, ^cfrmarcos@icv.csic.es, ^dmcastro@fi.mdp.edu.ar

Keywords: piezoelectric ceramics, lead-free compositions, ferroelectric properties.

Abstract. Different processing conditions and the effect of secondary phases on ferroelectric properties of $\text{Bi}_{0.5}(\text{Na}_{0.8}\text{K}_{0.2})_{0.5}\text{TiO}_3$ (BNKT) were studied. Ceramic powders were prepared by solid state reaction and different sintering conditions (1075 to 1100°C) were analyzed. Finally, samples were characterized by X-ray diffraction, Raman microspectroscopy, Scanning Electron Microscopy, impedance spectroscopy, and density measurements. Through XRD patterns, the perovskite structure was stabilized, together small peaks corresponding to a secondary phase associated with $\text{K}_{2-x}\text{Na}_x\text{Ti}_6\text{O}_{13}$. Moreover, the content of the secondary phase, d_{33} piezoelectric constant and dielectric properties increased with the sintering temperature.

Introduction

Lead titanate–zirconate piezoceramics are the most important and widely used materials for piezoelectric transducers, transformers and sensors. They have played a dominant role in the piezoelectrics field for a long time because of their excellent piezoelectric properties [1]. However, the toxicity of lead is a serious threat to human health and environment [2]. Thus, considerable effort has been devoted towards the development of lead-free piezoelectric ceramics.

Numerous studies on lead-free piezoelectric ceramics, such as (K,Na)NbO₃, BaTiO₃-based, Bi-layered, bismuth sodium titanate and tungsten bronze-type materials, have been recently published. For this reason, K_{0.5}Na_{0.5}NbO₃ (KNN) system attracts much attention, for its elevated Curie temperature (about 420°C) and high piezoelectric properties close to the morphotropic phase boundary (MPB) [3]. However, it is difficult to obtain pure KNN ceramics with high density and great piezoelectric performance. Sodium bismuth titanate Na_{0.5}Bi_{0.5}TiO₃ (BNT) with a relatively large remanent polarization at room temperature and a relatively high Curie temperature, could be considered another promising candidate of lead-free piezoelectric ceramics. However, its high coercive field hinders the obtention of the desired piezoelectric properties. Therefore, a number of studies have been carried out to improve electrical properties of BNT by the formation of solid solutions with other ABO₃ perovskites [4-5]. It has been reported that BNT ceramics modified with Bi_{0.5}K_{0.5}TiO₃ (BKT) showed improved dielectric and piezoelectric properties, due to a rhombohedral–tetragonal morphotropic phase boundary (MPB) at the optimal composition of Bi_{0.5}(Na_{0.85}K_{0.15})_{0.5}TiO₃ [6].

In the current work, lead-free Bi_{0.5}(Na_{0.8}K_{0.2})_{0.5}TiO₃-based ceramics were prepared by the solid state reaction method using a previous mechanochemical activation step of reagents. Results were discussed considering the effect of secondary phases on structure, microstructure, dielectric and piezoelectric properties of these ceramics.

Experimental Procedure

Bi_{0.5}(K_{0.2}Na_{0.8})_{0.5}TiO₃ was synthesized through solid state reaction, using K₂CO₃ and Na₂CO₃ (Cicarelli 99,99%; Argentina), Bi₂O₃ (Aldrich 99,8%; USA) and TiO₂ (Aldrich 99,9%; USA). Powders were mixed and milled using zirconia balls in alcoholic medium for 5 h in a planetary mill (Fritsch, Pulverisette 7, 1450 rpm). Powders were dried and calcined at 700°C for

2 h. The calcined powders were milled again, pressed into disks and sintered at 1075 to 1150°C for 2 h.

Crystalline phases were characterized by X-ray diffraction (XRD) (Philips PW1830), using CuK α radiation. Raman spectra were acquired at room temperature with a Renishaw inVia microscope by means of the 514 nm Ar-ion laser line (50 mW nominal power) with a diffraction grating of 2400 lines/mm. Density values were determined using the Archimedes method. Microstructures were evaluated on polished and thermally etched samples using a Field Emission Scanning Electron Microscope, FE-SEM (Hitachi S-4700). Previous to the electrical measurements, a fired silver paste was used for the electric contacts. Dielectric properties were determined at different frequencies using impedance analyzers Hioki 3532-3550 in the frequency range 100 mHz-10 MHz at room temperature. Samples were polled in a silicon oil bath at 25°C by applying a DC field of 30.0 kV/cm for 30 min. The piezoelectric constant d_{33} was measured using a piezo d_{33} meter (YE2730A d_{33} METER, APC International, Ltd., USA). Finally, the ferroelectric nature of these ceramics was determined using a hysteresis meter (RT 6000 HVS, RADIANT Technologies).

Results and Discussion

From XRD patterns (Fig. 1), the BNKT phase was stabilized in all sintered samples. However, samples sintered at temperatures higher than 1100°C presented secondary phases, which can be indexed to $K_{2-x}Na_xTi_6O_{13}$ phase (monoclinic structure, JCPDS Nos. 40-0403 and 74-0275).

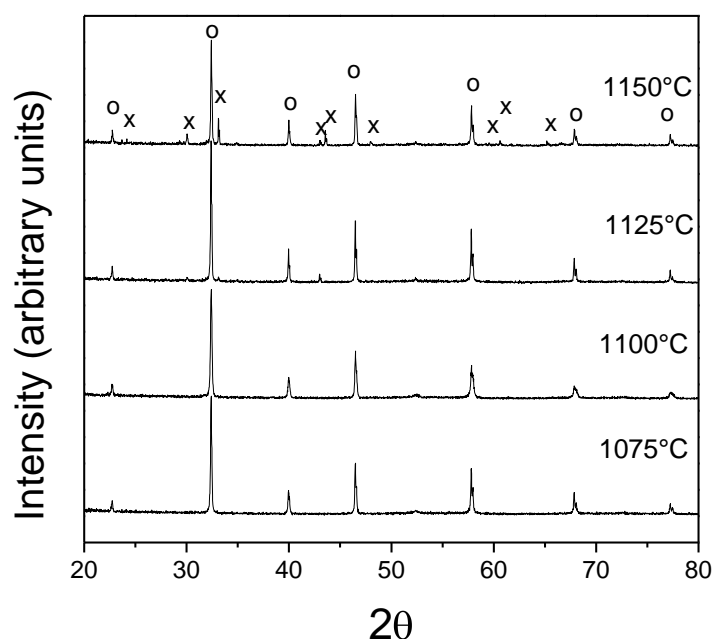


Figure 1. XRD patterns of sintered samples. (o) Peaks corresponding to BNKT phase, (x) peaks associated with a secondary phase.

Raman analyses were performed on different regions of all sintered samples between 200 and 1000 cm^{-1} (Fig. 2). From Raman spectra, six vibration bands corresponding to BNKT, in all sintered samples were observed. The amplitude and overlapping Raman bands reflected the strong anharmonicity and disorder inherent to A-sites. Moreover, new peaks related to a secondary phase assigned to $K_{2-x}Na_xTi_6O_{13}$ were observed. Peaks below 500 cm^{-1} could be attributed to the K–O–Ti stretching vibration. Peaks at about 655 cm^{-1} have been assigned to the Ti–O–Ti stretch in edge-shared TiO_6 . Peaks near 870 cm^{-1} were reported for a short Ti–O stretching vibration in distorted TiO_6 . Weak peaks around 240 and 400 cm^{-1} characteristic of the K–O–Ti containing short Ti–O bonds were also observed. Although secondary phases were not

detected through XRD patterns at the lowest sintering temperature, Raman spectra confirmed the formation of a secondary phase with composition close to $K_{2-x}Na_xTi_6O_{13}$ in all samples [7].

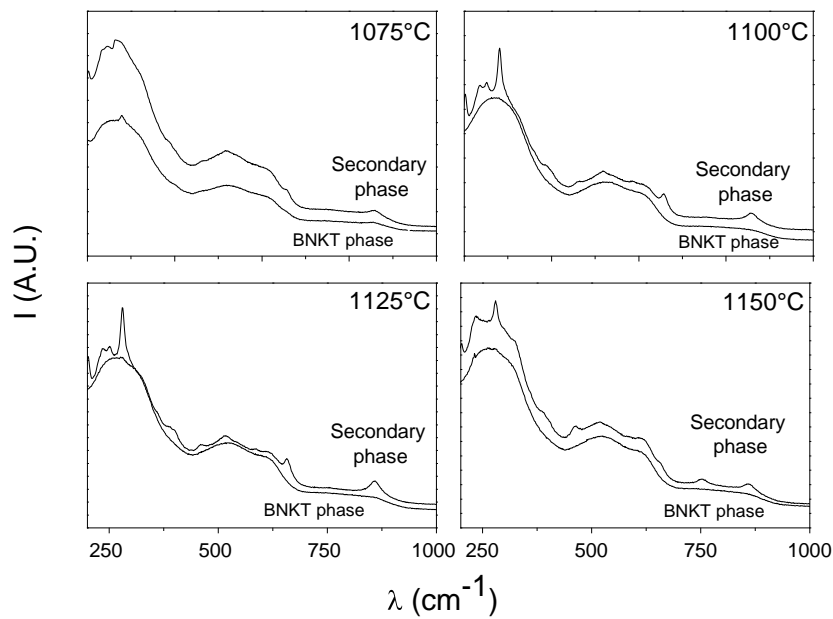


Figure 2. Raman spectra of sintered samples.

Microstructural characteristics of sintered samples were observed through Field Emission Scanning Electron Microscopy (FE-SEM) (Fig. 3). The FE-SEM micrographs showed the typical BNKT morphology consisting of faceted grains with a very small grain size. Furthermore, it was determined that sintering temperature affected the grain size and the amount of secondary phases. A secondary phase was also detected in the form of rods, probably due to the formation of $K_{2-x}Na_xTi_6O_{13}$, as detected by XRD and Raman microspectroscopy. All systems show small grains ($\leq 1 \mu m$) that become finer at low sintering temperatures.

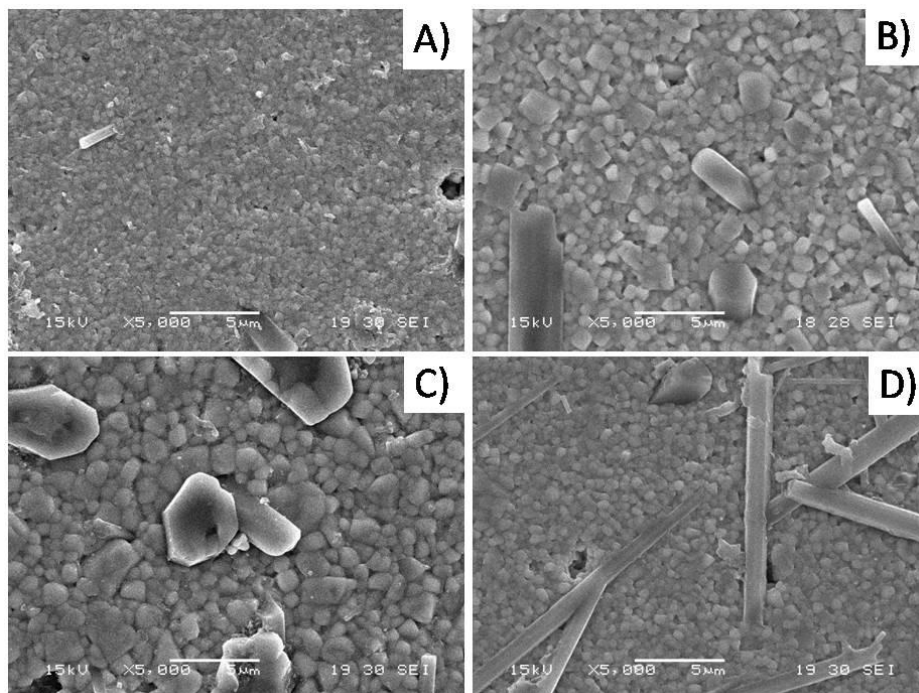


Figure 3. FE-SEM images of pure BNKT sintered at (A) 1075°C, (B) 1100°C, (C) 1125°C and (D) 1150°C.

Relative permittivity and dielectric loss values as a function of frequency for samples sintered at different temperatures were measured at room temperature (Fig. 4). In all cases, it was determined that at low frequencies, permittivity decreases drastically due to a space charge relaxation process characteristic of the polycrystalline material. Additionally, a relaxation process at high frequency (8-MHz) which was associated with a dipolar relaxation phenomena was observed. In these samples, the improvement in the real permittivity value with the sintering temperature could be related to the secondary phase formation and the densification degree.

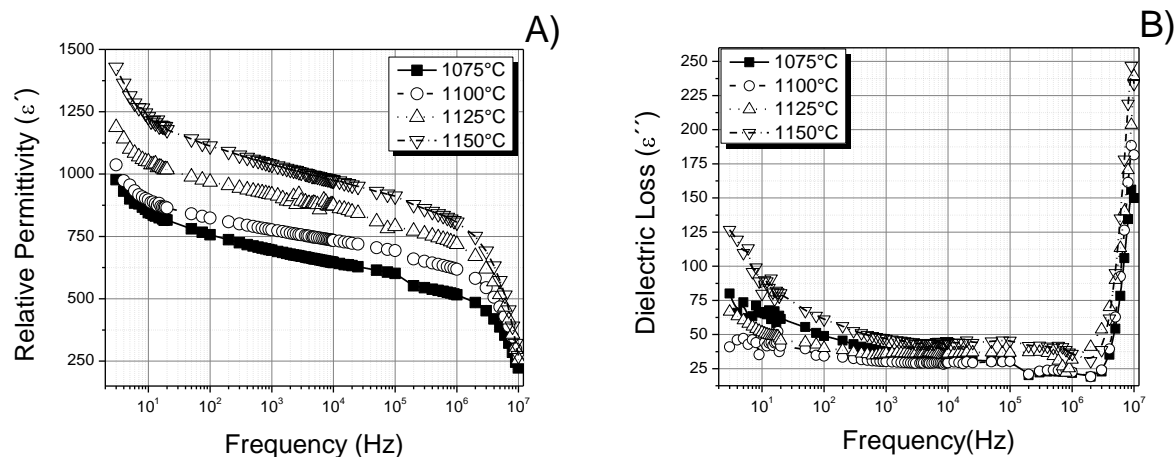


Figure 4. Curves of relative permittivity (A) and dielectric loss (B) as a function of frequency at room temperature.

From density measurements, samples sintered at 1100°C presented the maximum value of the complete set of samples (Table 1). Interestingly, the higher the sintering temperature, the higher the piezoelectric constant (d_{33}) and real permittivity values (Table 1). Although this secondary phase was not previously reported in BNKT systems, according to these observations the presence of this secondary phase contributes to the improvement of the ferroelectric and piezoelectric properties of BNKT-based ceramics. The apparition of this phase could be related with the mechanochemical activation of the powders in the solid state reaction method.

Table 1. Density, real permittivity (ϵ'), dielectric loss (ϵ''), and piezoelectric constant (d_{33}) values of the sintered samples.

Sintering temperature (°C)	Density (g/cm ³)	ϵ'	ϵ''	d_{33} (pC/N)
1075	5.64	674	33.8	30
1100	5.79	760	29.5	50
1125	5.65	879	36.8	90
1150	5.59	1014	43.9	100

Finally, hysteresis loops of sintered samples were collected at room temperature (Fig. 5). BNKT sintered at 1075°C showed a remnant polarization (P_r) 1.31 $\mu\text{C}/\text{cm}^2$, which increased to 2.13, 3.09 and 9.54 $\mu\text{C}/\text{cm}^2$ with the sintering temperature rising. The coercive electric field (E_c), and the saturation polarization values (P_s) were 9.63, 16.59, 15.58 and 25.1 kV/cm and for samples sintered at 1075, 1100, 1125 and 1150°C, respectively. Taking into account the increase in the coercive electric field values, a hardness effect on the ferroelectric properties of BNKT with the increase of sintering temperature was detected. This result could be associated with the secondary phase amount, the densification degree, and the anchoring effect of grain boundaries which limit the polarization of material and increase the coercive field of the samples and the energy involved in changing the polarization of the material.

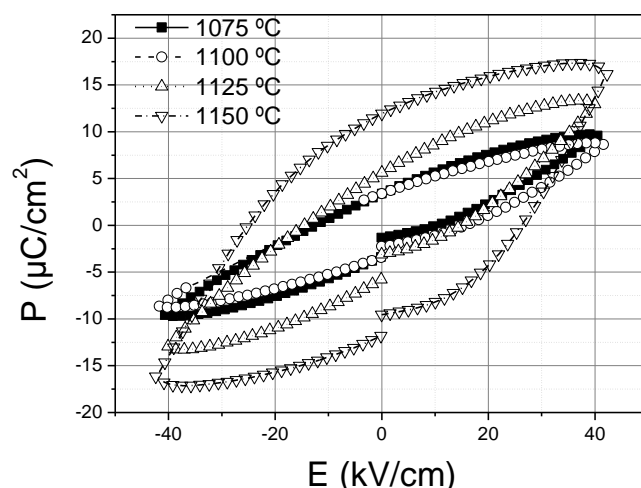


Figure 5. Hysteresis loops at room temperature of sintered ceramics.

Summary

The effect of sintering temperature on the microstructure, secondary phase formation and electric properties of $\text{Bi}_{0.5}(\text{Na}_{0.8}\text{K}_{0.2})_{0.5}\text{TiO}_3$ (BNKT)-based ceramics obtained by the conventional mixed oxide method has been reported. The formation of main perovskite type structure and a secondary phase which composition close to $\text{K}_{2-x}\text{Na}_x\text{Ti}_6\text{O}_{13}$ were detected. The amount of this secondary phase was increased with the sintering temperature. Interestingly, this secondary phase improved the piezoelectric properties and the remnant polarization of these ceramics.

References

- [1] B. Jaffe, W. R. Cook, and H. Jaffe, *Piezoelectric ceramics*, Academic Press, London, 1971.
- [2] J. Rodel, W. Jo, K. T. P. Seifert, E. M Anton, T. Granzow, D. Damjanovic, Perspective on the development of lead-free piezoceramics, *J. Am. Ceram. Soc.* 92 (2009) 1153-1177.
- [3] R. Wang, R. Xie, T. Sekiya, Y. Shimojo, Fabrication and characterization of potassium-sodium niobate piezoelectric ceramics by spark-plasma-sintering method, *Mater. Res. Bull.* 39 (2004) 1709-1715.
- [4] D. Lin, K.W. Kwok, H.L.W. Chan, Structure and electrical properties of $\text{Bi}_{0.5}\text{Na}_{0.5}\text{TiO}_3$ – BaTiO_3 – $\text{Bi}_{0.5}\text{Li}_{0.5}\text{TiO}_3$ lead-free piezoelectric ceramics, *Solid State Ionics*, 178 (2008) 1930-1937.
- [5] M. Jiang, X. Liu, C. Liu, Effect of BiFeO_3 additions on the dielectric and piezoelectric properties of $(\text{K}_{0.44}\text{Na}_{0.52}\text{Li}_{0.04})(\text{Nb}_{0.84}\text{Ta}_{0.1}\text{Sb}_{0.06})\text{O}_3$ ceramics, *Mater. Res. Bull.*, 45 (2010) 220-223.
- [6] B. Wang, L. Luo, F. Ni, P. Du, W. Li, H. Chen, Piezoelectric and ferroelectric properties of $(\text{Bi}_{1-x}\text{Na}_{0.8}\text{K}_{0.2}\text{La}_x)_{0.5}\text{TiO}_3$ lead-free ceramics, *J. Alloys Compd.*, 526 (2012) 79-84.
- [7] X. Meng, D. Wang, J. Liu, B. Lin, Z. Fu, Effects of titania different phases on the microstructure and properties of $\text{K}_2\text{Ti}_6\text{O}_{13}$ nanowires, *Solid State Commun.*, 137 (2006) 146–149.